Information-preserving pseudo-enhancement correction for non-cathartic low-dose dual-energy CT colonography

(Article begins on next page)

25 September 2024

Information-Preserving Pseudo-Enhancement Correction for Non-Cathartic Low-Dose Dual-Energy CT Colonography

Janne J. Näppi[1], **Rie Tachibana**[1], **Daniele Regge**[2], and **Hiroyuki Yoshida**[1]

[1]3D Imaging Research, Department of Radiology, Massachusetts General Hospital and Harvard Medical School, 25 New Chardon Street, Suite 400C, Boston, MA 02114, USA

[2]Institute for Cancer Research and Treatment, Candiolo Str. Prov. 142, 10060 Turin, Italy

Abstract

In CT colonography (CTC), orally administered positive-contrast fecal-tagging agents can cause artificial elevation of the observed radiodensity of adjacent soft tissue. Such pseudo-enhancement makes it challenging to differentiate polyps and folds reliably from tagged materials, and it is also present in dual-energy CTC (DE-CTC). We developed a method that corrects for pseudo-enhancement on DE-CTC images without distorting the dual-energy information contained in the data. A pilot study was performed to evaluate the effect of the method visually and quantitatively by use of clinical non-cathartic low-dose DE-CTC data from 10 patients including 13 polyps covered partially or completely by iodine-based fecal tagging. The results indicate that the proposed method can be used to reduce the pseudo-enhancement distortion of DE-CTC images without losing material-specific dual-energy information. The method has potential application in improving the accuracy of automated image-processing applications, such as computer-aided detection and virtual bowel cleansing in CTC.

Keywords

CT colonography; Pseudo-enhancement; Dual-energy CT; Virtual colonoscopy

1 Introduction

Computed tomographic colonography (CTC) uses orally administered positive-contrast fecal-tagging agents for opacifying residual fluid and feces on CTC images. The expectation is that, because fecal-tagged fluid and feces should have high CT values of >100 Hounsfield units (HU) on CTC images, they can be differentiated reliably from the CT values of soft-tissue lesions (approximately 0 – 100 HU). However, if the fecal-tagging agent has high radiodensity (>300 HU), it tends to cause artificial local elevation of the CT values of adjacent soft-tissue lesions and haustral folds. This makes reliable visualization and automated detection of lesions challenging, because CT values of >100 HU may now indicate both lesions and tagged fecal materials [1].

Previously, an automated image-based pseudo-enhancement correction (PEC) method was developed for single-energy CTC [1]. Studies have shown that the application of PEC can improve the performance of automated polyp detection [2] and electronic cleansing [3]. Later approaches have included a scale-based scatter correction method [4] and a non-linear correction method [5].

Recently, dual-energy CTC (DE-CTC) has been used to improve the accuracy of image-processing applications over conventional single-energy CTC, because it can provide quantitative material-specific measurements for differentiating fecal tagging and partial-volume artifacts from soft-tissue lesions more precisely than does single-energy CTC which only provides intensity information [6,7]. However, pseudo-enhancement is still present on dual-energy CTC (DE-CTC) images, which are typically acquired at 140 kVp and 80 kVp energy levels. This can degrade the ability of DE-CTC to differentiate reliably between materials.

The PEC methods of single-energy CTC cannot be applied directly to DE-CTC images, because this would distort the dual-energy information (Fig. 1). Therefore, in this study, we developed an information-preserving method for performing PEC on DE-CTC images. A preliminary evaluation of the method was performed by use of clinical non-cathartic low-dose DE-CTC cases.

2 Materials and Methods

2.1 Materials

Ten patients were prepared for a non-cathartic CTC examination by oral ingestion of 50 ml of iodinated contrast agent (Gastrografin, Therapex, Canada) on the day before and two hours prior to CT acquisitions by a dual-energy CT scanner (SOMATOM Definition Flash, Siemens Healthcare, Germany). The CT acquisitions were performed in supine and prone positions at 15 mA for the 140 kVp scan and at 40 mA for the 80 kVp scan. The average CT dose index by volume was 0.95 mGy and the effective dose was 0.75 mSv per CT scan volume. The dual-energy images were constructed by use of a sinogram-affirmed iterative image reconstruction (SAFIRE) algorithm [8, 9] at 0.6 – 1.0 mm reconstruction intervals. The locations of 13 clinically significant polyps (6 mm in largest diameter) that were confirmed by same-day colonoscopy were correlated with the CTC images by a radiologist with extensive experience on interpreting CT colonography (>1000 cases read).

2.2 Pseudo-Enhancement Correction (PEC1) for Single-Energy CTC

Because the dual-energy PEC method is based in part upon a single-energy PEC method, we will briefly discuss the basic idea of the latter. In the remainder of this text, we will denote this single-energy method as PEC1 and its dual-energy version as PEC2.

In the PEC1-method [1], pseudo-enhancement is modeled as a process of iterative enhancement that radiates three-dimensionally from voxels with high CT value into their surrounding voxels, thereby causing increment in the observed CT values of the surrounding voxels. More precisely, if v_p denotes the correct CT value at voxel p, and $\tilde{v}_p$ denotes the observed pseudo-enhanced CT value, the observed CT value is modeled as

$$\tilde{v}_p = v_p + \delta_p, \quad (1)$$

where δ_p denotes the effect of pseudo-enhancement at p. The value of δ_p is estimated by use of an iterative algorithm. First, we assume that each voxel with a high CT value distributes some amount of initial pseudo-enhancement energy to its adjacent voxels. At a voxel q, the initial pseudo-enhancement energy is approximated as $e_q = \max\{0, \ \tilde{v}_q - \tau_q\}$, where τ_q is a parameter threshold for the smallest CT value that is considered to cause pseudo-enhancement.

At the first iteration, e_q is distributed to the surrounding voxels according to a 3-D Gaussian field function. Each affected voxel receives some pseudo-enhancement energy from its surrounding voxels. Let $r^0(p)$ denote the total pseudo-enhancement energy received by voxel p at the first iteration.

At subsequent iterations, the pseudo-enhancement energy that was received by voxel p at the previous iteration is redistributed to the surrounding voxels (Fig. 2(a)). Simultaneously, the total pseudo-enhancement energy that has been received by p is being accumulated at p. Let $r^i(p)$ denote the pseudo-enhancement energy that was received by p at ith iteration.

The iterations continue, until the distributable pseudo-enhancement energy becomes negligible, i.e. when the effect of the largest pseudo-enhancement energy received by a voxel drops to less than 1 HU. The iterations converge, because the total distributed pseudo-enhancement energy is reduced at each iteration. From Eq. (1), the pseudo-enhancement correction for a voxel p is calculated as

$$v_p = \tilde{v}_p - \delta_p = \tilde{v}_p - \sum_{i=0}^{m} r^i(p), \quad (2)$$

where m is the number of completed iterations. After the application of Eq. (2), pseudo-enhanced soft-tissue lesions can be seen in a soft-tissue display window (Fig. 2(b)).

The method was calibrated by use of an anthropomorphic phantom that was filled partially with three radio-densities of diluted iodine corresponding to observed CT values of 300 HU, 600 HU, and 900 HU. The CT acquisitions were performed at 140 kVp tube voltage and 50 mA current with an eight-channel CT scanner (LightSpeed Plus, GE Medical Systems, Milwaukee, WI, USA) using a 2.5-mm collimation and 1.8-mm reconstruction interval. The calibration involved the optimization of two parameter functions that provide the radius of the Gaussian distribution field as a function of e_q and r^i, respectively. The objective function was the observed difference of CT values in the three partially filled phantoms in comparison with an empty phantom [1].

2.3 Information-Preserving Pseudo-Enhancement Correction (PEC2) for DE-CTC

To perform dual-energy PEC, first we use the PEC1 method of Sect. 2.2 to correct the 140 kVp image of the dual-energy image pair independently from the 80 kVp image. Next, we correct the 80 kVp image according to

$$v_{80} = \frac{v_{140}}{\tilde{v}_{140}} \tilde{v}_{80}, \quad (3)$$

where v_{80} is the corrected CT value, v_{140} and $\tilde{v}_{140}$ are the PEC1-corrected and uncorrected CT values of the 140 kVp image, respectively, and $\tilde{v}_{80}$ is the uncorrected CT value of the 80 kVp image.

It is easy to see that Eq. (3) preserves the dual-energy image information. For the dual-energy ratio (DER) feature, from Eq. (3) we have

$$\text{DER} = \frac{v_{140}}{v_{80}} = \frac{v_{140}\tilde{v}_{140}}{v_{140}\tilde{v}_{80}} = \frac{\tilde{v}_{140}}{\tilde{v}_{80}}. \quad (4)$$

The dual-energy index (DEI) feature is calculated as [10]

$$\text{DEI} = \frac{v_{80} - v_{140}}{v_{80} + v_{140} + 2000}. \quad (5)$$

From Eq. (3), we have

$$\text{DEI} = \frac{\tilde{v}_{140}(v_{140}\tilde{v}_{80} - v_{140}\tilde{v}_{140})}{v_{140}\tilde{v}_{80} + v_{140}\tilde{v}_{140} + \tilde{v}_{140}2000} = \frac{\tilde{v}_{80} - \tilde{v}_{140}}{\tilde{v}_{80} + \tilde{v}_{140} + \frac{\tilde{v}_{140}}{v_{140}}2000}. \quad (6)$$

Thus, to preserve the value of DEI after the correction, it would be necessary to adjust the constant 2000 in the denominator relative to the correction of the 140 kVp image at each point.

2.4 Evaluation Methods

For a pilot study, we evaluated the PEC2-method both visually and quantitatively by use of the 20 DE-CTC scan pairs (see Sect. 2.1). For visual evaluation, we calculated water-iodine basis decomposition images and virtual monochromatic images (VMIs) [11] from uncorrected and PEC2-corrected 140 kVp and 80 kVp energy images. For quantitative evaluation, we calculated the mean CT values of polyps covered partially or completely by fecal tagging in 100 keV and 120 keV VMIs without and with the application of PEC2. The CT values of each polyp were sampled from the center voxel and its 6-neighborhood voxels.

To calculate VMIs, we solved the material fractions from [11]

$$\begin{pmatrix} \mu_1 \\ \mu_2 \end{pmatrix} = \begin{pmatrix} M_1 \\ M_2 \end{pmatrix} \times \begin{pmatrix} \frac{\mu}{\rho_1}(E) \times \rho_1 \\ \frac{\mu}{\rho_2}(E) \times \rho_2 \end{pmatrix}, \quad (7)$$

where μ_1 and μ_2 are the observed linear attenuation coefficient values, M_1 and M_2 are the material fractions, ρ_1 and ρ_2 are the material densities, and $\frac{\mu}{\rho_1}$ and $\frac{\mu}{\rho_2}$ are the mass attenuation

coefficients at an average energy *E*. After solving of the material fractions, the VMI is calculated by reapplication of Eq. (7) at the desired monochromatic energy *E*.

3 Results

Figures 3(a) and (b) show an example of the water-iodine basis image decomposition with pseudo-enhancement correction by the PEC2 method for the same region as that of Fig. 1. The presence of iodine (tagging agent) is now indicated correctly by the iodine image (Fig. 3(b)). Figure 3(c) shows the corresponding VMI calculated at 120 keV.

Figure 4 demonstrates the effect of the adjustment term $\frac{\tilde{v}_{140}}{v_{140}}$ of Eq. (6). The use of original DEI of Eq. (5) yields differences between DEI images calculated from the uncorrected and PEC2-corrected dual-energy images (Fig. 4(a)), whereas the use of adjusted DEI of Eq. (6) yields identical values (Fig. 4(b)).

Figure 5 shows a comparison of the CT values within polyps sampled from VMIs calculated at 100 keV and 120 keV energies from the uncorrected and PEC2-corrected dual-energy images. Each point represents the CT value of a voxel within a polyp. The measurements indicate that the PEC2 method is able to reduce pseudo-enhancement of the CT values of polyps without affecting the CT values of polyps that are not pseudo-enhanced.

Table 1 shows measurements of the average CT value of polyps in VMIs before and after the application of the PEC2 method. As expected, the correction is largest for small polyps and for those covered by fecal tagging. Because of the small number of samples (*n*), we did not estimate statistical significance.

4 Discussion

Pseudo-enhancement is considered to originate largely from the combined effect of x-ray scattering, beam hardening, and their inappropriate correction by commercial CT scanners [12]. Although the proprietary algorithms of CT scanners are probably attempting to correct for conventional beam-hardening effects, they have not been designed to correct for the variable presence of fecal-tagging contrast agents in CTC [1,13].

Previously, the use of retrospective image-based pseudo-enhancement correction methods was shown to reduce pseudo-enhancement and to improve the performance of automated image-processing methods in single-energy CTC. The preliminary results of this study indicate potentially similar benefits in DE-CTC by the application of the proposed PEC2 method. The method was shown to preserve material-specific information in terms of two key features that are used commonly in image-based material-specific analyses: the DER and DEI features.

On VMIs that were reconstructed by use of PEC2-corrected images, the results indicate similar trends than those observed previously in the correction of single-energy CTC images. The PEC does not affect the CT values of polyps that were not affected by pseudo-enhancement, but it does reduce the observed CT values of pseudo-enhanced polyps. The correction becomes larger as the effect of pseudo-enhancement increases (Fig. 5). The

quantitative measurement results showed that the correction is largest for polyps submerged in fecal tagging and for small polyps, and that after the correction the average CT values of polyps are within the expected soft-tissue range (Table 1).

Recent efforts to reduce the theoretical risks of medical radiation have resulted in efforts to minimize radiation dose in CTC examinations [14]. The iterative SAFIRE algorithm that we used in this study enables the use of low effective CT dose without compromising diagnostic image quality. However, the algorithm does not completely compensate for pseudo-enhancement which can be seen especially at the 80 kVp energy CT images. The proposed PEC2-method can be used to reduce such artifacts.

The DE-CTC data of this study were acquired by use of a non-cathartic CTC protocol. Bowel preparation has been identified as one of the major obstacles to colorectal screening. The use of non-cathartic or completely laxative-free [15–17] bowel preparation could provide substantial increment in patient adherence to colorectal screening guidelines [18].

This study had several limitations. First, the PEC2-method is based on a single-energy PEC1-method that was optimized for a different CT scanner by a different manufacturer than that used in our study. Previous studies have shown great variability when CT data are compared between different brands and models of scanners [19,20]. Therefore, a more accurate pseudo-enhancement correction can be expected if the method was optimized for the particular CT scanner and acquisition parameters used in a study. Second, the number of samples was small. Third, we did not perform a phantom study, where the exact CT values of target materials would be known. Nevertheless, the quantitative experiments indicate that the proposed PEC2 method can indeed be used to restore the expected soft-tissue CT values of pseudo-enhanced polyps on DE-CTC images without distorting the dual-energy information.

5 Conclusion

We developed a pseudo-enhancement correction method for dual-energy CT colonography. Preliminary evaluation indicates that the method is able to reduce pseudo-enhancement in dual-energy data while preserving the material-specific information of dual-energy images. The method has potential to improve the accuracy of material-specific analysis and automated image processing of dual-energy CTC images.

Acknowledgments

References

1. Näppi J, Yoshida H. Adaptive correction of the pseudo-enhancement of CT attenuation for fecal-tagging CT colonography. Med Image Anal. 2008; 12:413–426. [PubMed: 18313349]

2. Näppi J, Yoshida H. Fully automated three-dimensional detection of polyps in fecal-tagging CT colonography. Acad Radiol. 2007; 25:287–300. [PubMed: 17307661]

3. Zhang H, Li L, Zhu H, Han H, Song B, Liang Z. Integration of 3D scale-based pseudo-enhancement correction and partial volume image segmentation for improving electronic colon cleansing in CT colonography. J Xray Sci Techol. 2014; 22:271–283.

4. Liu J, Yao J, Summers R. Scale-based scatter correction for computer-aided polyp detection in CT colonography. Med Phys. 2008; 35:5664–5671. [PubMed: 19175123]

5. Tsagaan B, Näppi J, Yoshida H. Nonlinear regression-based method for pseudoenhancement correction in CT colonography. Med Phys. 2009; 36:3596–3606. [PubMed: 19746794]

6. Näppi, J.; Kim, S.; Yoshida, H. Automated detection of colorectal lesions with dual-energy CT colonography. In: van Ginneken, B.; Novak, C., editors. SPIE Medical Imaging 2012: Computed-Aided Diagnosis. Vol. 8315. 2012. p. 83150Y1-83150Y6.

7. Näppi, J.; Kim, S.; Yoshida, H. Volumetric detection of colorectal lesions for non-cathartic dual-energy computed tomographic colonography. Conference Proceedings of IEEE Engineering in Medicine and Biology Society; 2012. p. 3740-3743.

8. Kalra M, Woisetschläger M, Dahlström N, Singh S, Linblom M, et al. Radiation dose reduction with sinogram affirmed iterative reconstruction technique for abdominal computed tomography. J Comput Assist Tomogr. 2012; 36:339–346. [PubMed: 22592621]

9. Grant, K.; Raupach, R. Technical report. Siemens; 2012. SAFIRE: sinogram affirmed iterative reconstruction.

10. Zachrisson H, Engström E, Engvall J, Wigström L, Smedby O, Persson A. Soft tissue discrimination ex vivo by dual energy computed tomography. Eur J Radiol. 2010; 75:e124–e128. [PubMed: 20219308]

11. Yu L, Leng S, McCollough C. Dual-energy CT-based monochromatic imaging. Am J Roentgenol. 2012; 199:S9–S15. [PubMed: 23097173]

12. Maki D, Birnbaum B, Chakraborty D, Jacobs J, Carvalho B, Herman G. Renal cyst pseudoenhancement: beam-hardening effects on CT numbers. Radiology. 1999; 213:468–472. [PubMed: 10551228]

13. Boas F, Fleischmann D. CT artifacts: causes and reduction techniques. Imaging Med. 2012; 4:229–240.

14. Chang K, Yee J. Dose reduction methods for CT colonography. Abdom Imaging. 2013; 38:224–232. [PubMed: 23229777]

15. Zalis M, Blake M, Cai W, Hahn P, et al. Diagnostic accuracy of laxative-free computed tomographic colonography for detection of adenomatous polyps in asymptomatic adults: a prospective evaluation. Ann Intern Med. 2012; 156:692–702. [PubMed: 22586008]

16. Lefere P, Gryspeerdt S, Baekelandt M, Van Holsbeeck B. Laxative-free CT colonography. Am J Roentgenol. 2004; 183:945–948. [PubMed: 15385285]

17. Johnson C, Manduca A, Fletcher J, MacCarty R, et al. Noncathartic CT colonography with stool tagging: performance with and without electronic stool subtraction. Am J Roentgenol. 2008; 190:361–366. [PubMed: 18212221]

18. Beebe T, Johnson C, Stoner S, Anderson K, Limburg P. Assessing attitudes toward laxative preparation in colorectal cancer screening and effects on future testing: potential receptivity to computed tomographic colonography. Mayo Clinic Proc. 2007; 82:666–671.

19. Grosjean R, Daudon M, Chammas M Jr, Claudon M, et al. Pitfalls in urinary stone identification using CT attenuation values: are we getting the same information on different scanner models? Eur J Radiol. 2013; 82:1201–1206. [PubMed: 23601294]

20. McCullough E. Factors affecting the use of quantitative information from a CT scanner. Radiology. 1977; 124:99–107. [PubMed: 866663]
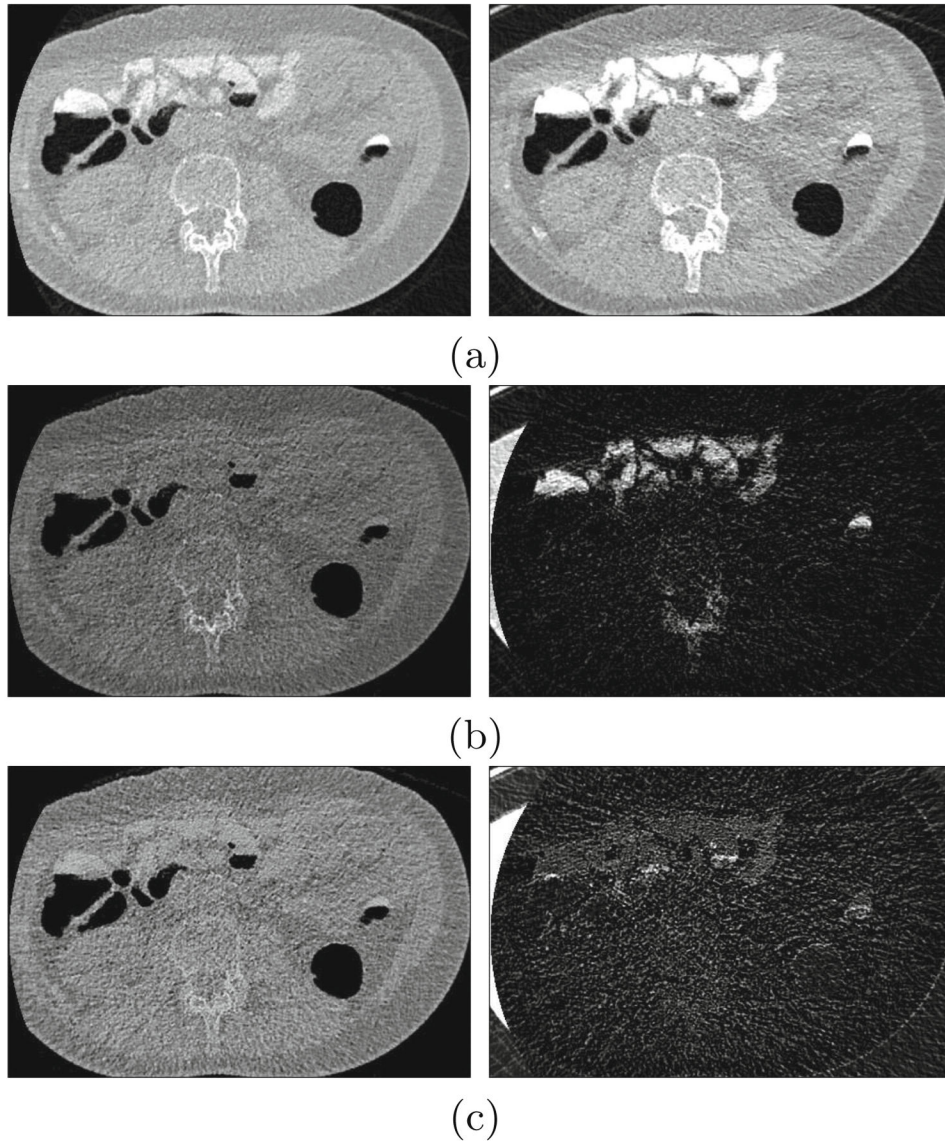
Fig. 1.
(a) An example of a 140 kVp and 80 kVp energy image pair. (b) The corresponding water-iodine basis material decomposition. (c) After performing a single-energy pseudo-enhancement correction independently on each energy image, the subsequent basis material decomposition indicates the presence of iodine incorrectly.
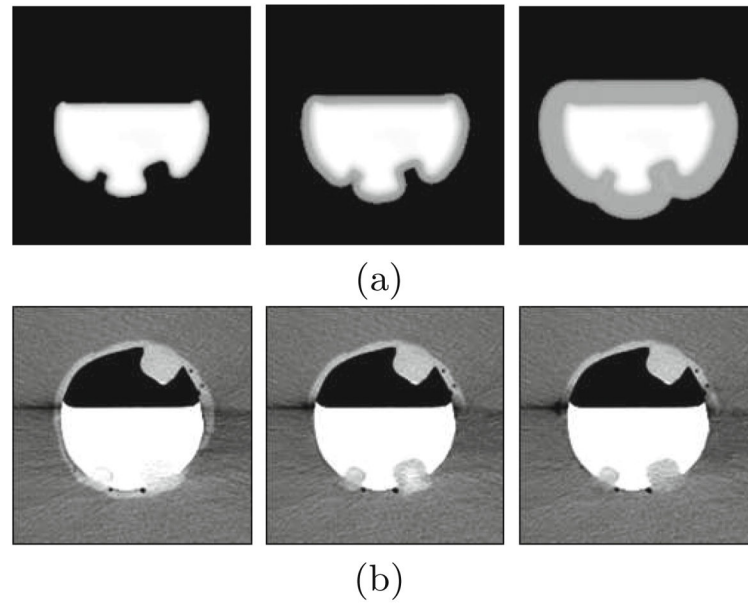
Fig. 2.
Illustration of the calculation of pseudo-enhancement correction. (a) A 2-D cut-plane view of the pseudo-enhancement correction field after 1, 10, and 20 iterations. (b) The corresponding corrected image shows how the CT values of two pseudo-enhanced polyps covered by tagged fluid are gradually corrected by the method.
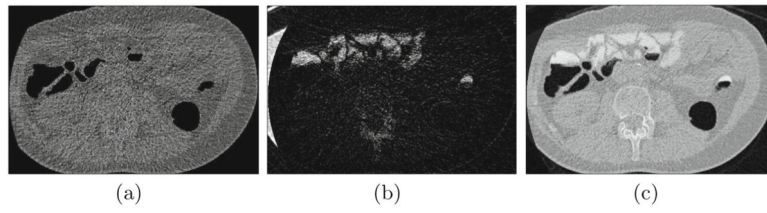
Fig. 3.
(a) Water and (b) iodine basis decomposition images calculated from the PEC2-corrected
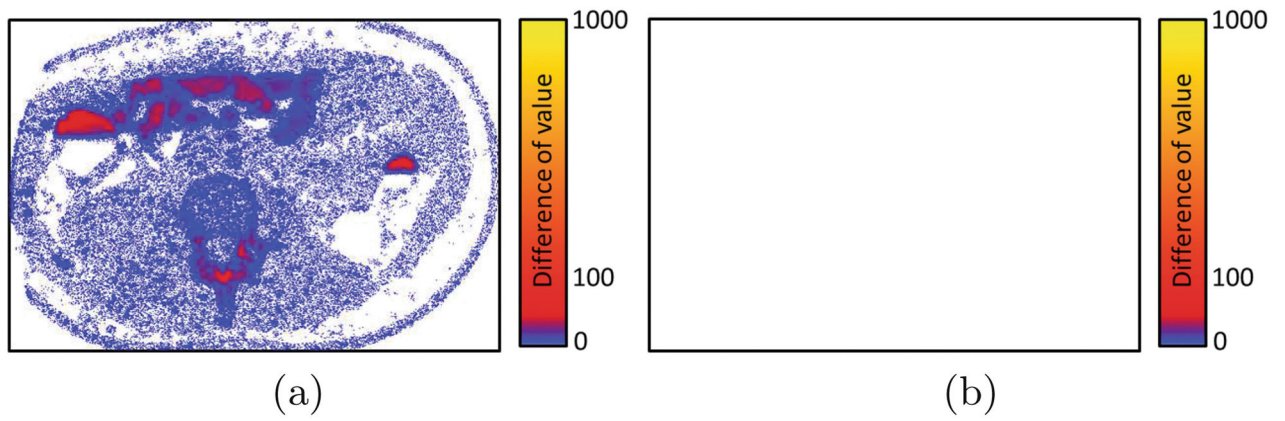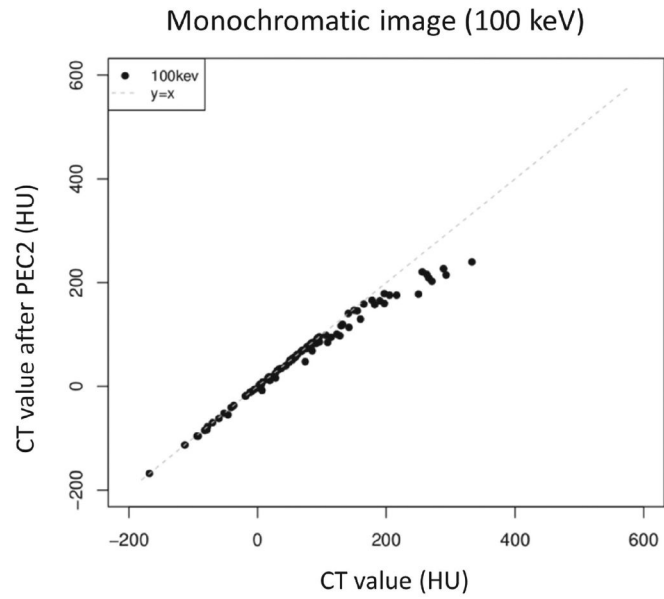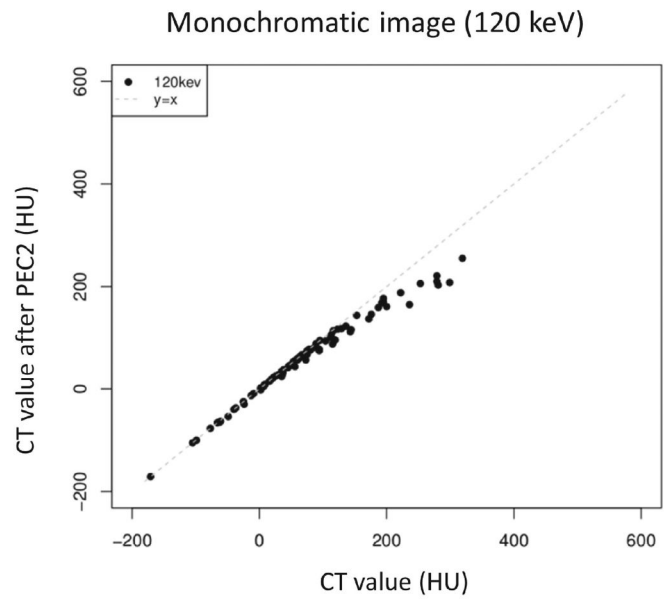140 kVp and 80 kVp input images. (c) VMI of the region at 120 keV.

Fig. 4.
Difference images of the DEI-feature calculated from the uncorrected and PEC2-corrected dual-energy images. White color indicates identical value, i.e., no difference. (a) Original DEI (Eq. (5)) indicates some differences. (b) Adjusted DEI (Eq. (6)) yields identical values (white color) with the original data.

Fig. 5.
Comparison of the CT values of VMIs calculated from uncorrected (x-axis) and PEC2-corrected (y-axis) dual-energy images, respectively, (a) at 100 keV and (b) at 120 keV.

Table 1

Measurements of the average CT values of polyps (in HU) on VMIs without and with the application of the PEC2 method.

E = 120 keV	n	Uncorrected	PEC2	Change
Small (6 – 9 mm)	3	72	47	−25
Large (10 mm)	10	70	62	−8
Partially covered	3	27	24	−3
Submerged	6	93	76	−17
E = 100 keV	n	Uncorrected	PEC2	Change
Small (6 – 9 mm)	3	57	33	−24
Large (10 mm)	10	76	68	−8
Partially covered	3	20	16	−4
Submerged	6	103	86	−17